Polynomial-Chaos Uncertainty Modeling in Eddy-Current Inspection of Cracks

T. T. Zygiridis[1*], A. E. Kyrgiazoglou[2], T. P. Theodoulidis[2]
1. Department of Informatics and Telecommunications Engineering, University of Western Macedonia, Kozani 50131, Greece
2. Department of Mechanical Engineering, University of Western Macedonia, Kozani 50132, Greece
*Karamanli & Lygeris, Kozani 50131, Greece (tzygiridis@uowm.gr)

Abstract: This paper investigates the forward problem of crack detection on conducting objects via eddy-current inspection in a stochastic framework. Unlike the majority of pertinent works that are suitable only for deterministic problems with precisely described parameters, we follow a line of work that takes into account potential uncertainties characterizing the geometric properties of the defects, which eventually influence the corresponding outcomes. As the implementation of standard techniques, such as the Monte-Carlo approach, require elongated simulation times (even of the order of days for 3D geometries), the suggested methodology alternatively derives polynomial-chaos expansions of the random quantities of interest by exploiting efficient sparse-grid quadrature rules, thus enabling significant reduction of the involved computational cost. The numerical results verify that, in this way, COMSOL® capabilities can be further expanded to provide reliable statistical characterization of eddy-current inspection problems with variability in their parameters.

Keywords: AC/DC module, crack detection, eddy-current testing, polynomial chaos, sparse grids, uncertainty quantification.

1. Introduction

Detection of defects, such as cracks, in metallic configurations via eddy-current inspection comprises an active research area of non-destructive evaluations with increasing interest [1, 2]. In essence, the presence of a crack can be identified by observing the perturbation of a coil's impedance, with respect to the case of the "flawless" structure, when the position of the coil changes in the vicinity of the crack. Due to the importance – from an engineering viewpoint – of the aforementioned problems, various approaches have been developed for the solution of the forward problem. The combination of the finite element method (FEM) and the boundary element method (BEM) is proposed for eddy-current problems in [3], adopting a formulation that depends on the magnetic vector potential **A** and the scalar potential φ. A boundary element approach is presented in [4] for handling ideal plane cracks (i.e. defects with negligible opening). The work of [5] considers the vector-potential boundary-integral approach for studying eddy-current interactions with cracks, and explores cases where the skin depth is small, compared to the characteristic size of the defects. In [6], the source terms for an integral equation to be solved around the crack is obtained by imposing the current density to be the opposite of the unperturbed one, so that a vanishing total current inside the crack region is ensured. A FEM that considers changes in the crack shape is derived in [7], while various developments of the BEM that enable the significant reduction of the computational time are presented in [8], in the case of narrow cracks. The work of [9] pertains to a revision of an existing boundary element model for ideal or narrow cracks, and [10] applies edge elements using COMSOL®, in the context of benchmark problems. Finally, the **A**-formulation for the eddy-current problem is thoroughly studied in [11], neglecting the crack thickness and applying the FEM.

The aforementioned methodologies assume that the parameters of the investigated problem, either geometric or electric, are known in an exact fashion. If, from a more realistic viewpoint, one or more key factors display a degree of randomness, then the quantities of interest (e.g. the change of the coil's impedance) become stochastic, and their reliable characterization requires more sophisticated treatment. Monte-Carlo (MC) methodologies provide a standard line of work that enables the extraction of the statistical properties of random quantities, as long as a significant amount of output samples is available [12]. The latter is necessary due to the slow conver-

gence of the algorithm. Evidently, when time-consuming simulations are required for obtaining these samples, MC solutions become computationally inefficient. Alternative techniques that exploit the representation of random quantities via polynomial series [13] have been proven to perform more efficiently than MC methods, especially when combined with other numerical schemes, e.g. sparse-grid integration [14]. In essence, such methodologies are known to provide reliable results by requiring significantly fewer samples than MC approaches in many cases, reducing the involved computational times.

In this paper, we are interested in the case of eddy-current inspection of cracks, when geometric uncertainties need to be taken into account. Till today, problems involving eddy currents are rarely dealt with in a stochastic framework (see, for example, [15] for the case of eddy currents in the human body). As we do not wish to limit the applicability of this approach by adopting common simplifications, such as assumptions of ideal or narrow cracks, FEM modeling via the COMSOL® software is exploited for the calculation of the coil's impedance change. Despite the relatively simple geometric setup, the fine geometric features of the cracks call for locally refined meshes, leading to non-trivial simulation times. Consequently, the need for computationally efficient calculations rules out MC methodologies, leading to more preferable solutions based on polynomial-chaos (PC) expansions [13]. Uncertainty quantification is performed here in a non-intrusive manner, by employing spectral projection for the calculation of the expansion coefficients, and adopting sparse-grid integration for the case of multiple stochastic inputs. Key statistical measures, such as the expected value and the standard deviation of the impedance change, can be easily computed considering only the expansion coefficients. As we show, the reliable description of the problem's statistical properties becomes possible with only a fraction of MC's computational cost. A series of numerical comparisons strongly suggest that, by carefully conducting FEM studies with the COMSOL® software, efficient solutions of stochastic problems involving eddy-current defect detection can be derived.

2. Problem Description

The considered eddy-current problems are commonly described in terms of the vector potential **A**, according to the following mathematical model:

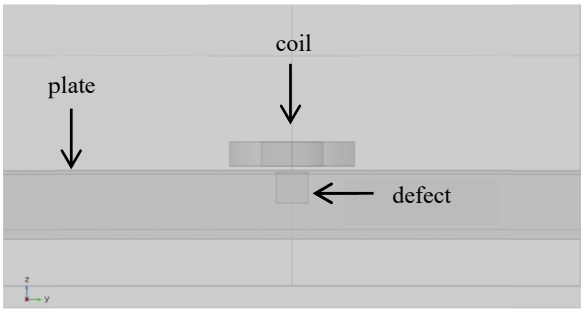

Figure 1. Typical problem configuration in eddy-current inspections: a coil over a crack in an aluminum plate.

$$\nabla\times\left(\frac{1}{\mu}\nabla\times\mathbf{A}\right)+\left(\mathrm{j}\omega\sigma-\omega^2\varepsilon\right)\mathbf{A}=\mathbf{J}_s \qquad (1)$$

where $\mathbf{J}_s$ stands for impressed current sources, ω is the angular frequency, σ is the conductivity, ε is the electric permittivity, μ is the magnetic permeability, and $\mathrm{j}=\sqrt{-1}$. For this type of studies, the AC/DC module of COMSOL is the most suitable choice for performing the necessary simulations. Regarding the boundary conditions, magnetic insulation is assumed at the enclosing boundaries of the computational domain, described by $\hat{\mathbf{n}}\times\mathbf{A}=\mathbf{0}$, where $\hat{\mathbf{n}}$ is the unit vector normal to the boundary.

As a representative test case, a 150mm × 150 mm × 10 mm aluminum plate (electric conductivity of 37.74 MS/m) is considered, with a $x_c \times y_c \times z_c$ crack positioned at its center point. The inner and outer radii of the 405-turn coil are selected as R_{in} = 5 mm, R_{out} = 10 mm, respectively. The coil's lift-off with respect to the plate is set to 1 mm, and its height is selected 4 mm. The coil is excited by a 10 kHz current, and the assigned density has the form

$$\mathbf{J}=J_0\frac{-y\hat{\mathbf{x}}+x\hat{\mathbf{y}}}{\sqrt{x^2+y^2}} \qquad (2)$$

where J_0 is the selected current density magnitude, calculated as the overall number of ampere-turns, divided by the area of the coil's vertical cross-section.

According to the eddy-current testing methodology, we need to record the changes in the coil impedance, when the position of the latter is modified with respect to the defect. Instead of altering the position of the coil, which necessitates the proper adjustment of the excitation current, the coil's movement can be equivalently taken into account by simply performing a similar change to the defect's position. Further-

more, two simulations are conducted for each placement and the coil's impedance with and without the presence of the defect is calculated. The impedance is derived via the integral

$$Z = \frac{j\omega}{I^2}\iiint_{V_c} \mathbf{A}\cdot\mathbf{J}dV \tag{3}$$

which is computed by COMSOL® (V_c stands for the volume occupied by the coil).

3. Polynomial-Chaos Models

In a completely deterministic context, the impedance change $\Delta Z = \Delta R + j\Delta X$ is normally a function of the coil position $\mathbf{r}$. If the problem is stochastic, then ΔZ becomes dependent on a number of d random variables (which are considered independent herein), represented by the vector $\boldsymbol{\xi} = [\xi_1\ \xi_2\ \ldots\ \xi_d]^T$. To facilitate the computation of the quantities of interest, truncated polynomial series are used for the representation of the change in the resistance and reactance ΔU, $U \in \{R, X\}$:

$$\Delta U(\mathbf{r},\boldsymbol{\xi}) \simeq \sum_{\ell=0}^{P} C_\ell^U(\mathbf{r})\Psi_\ell(\boldsymbol{\xi}) \tag{4}$$

In (4), $C_\ell^U(\mathbf{r})$ are expansion coefficients that depend on the coil position only, $\Psi_\ell(\boldsymbol{\xi})$ are multivariate polynomial functions, and $P + 1$ is the number of the expansion terms, determined by

$$P+1 = \frac{(p+d)!}{p!\,d!} \tag{5}$$

where p is the selected polynomial order of the series approximation. The Ψ functions are constructed as products of univariate expressions,

$$\Psi_\ell(\boldsymbol{\xi}) = \psi_{\alpha_1^\ell}(\xi_1)\cdot\psi_{\alpha_2^\ell}(\xi_2)\cdot\ldots\cdot\psi_{\alpha_d^\ell}(\xi_d) \tag{6}$$

where

$$\alpha_1^\ell + \alpha_2^\ell + \ldots + \alpha_d^\ell = \left|\boldsymbol{\alpha}^\ell\right| \le p \tag{7}$$

Furthermore, the $\Psi_\ell(\boldsymbol{\xi})$ functions form an orthogonal basis, with respect to the inner product

$$\left\langle f(\boldsymbol{\xi}), g(\boldsymbol{\xi})\right\rangle = \int_{\Omega^d} f(\boldsymbol{\xi})g(\boldsymbol{\xi})p(\boldsymbol{\xi})d\boldsymbol{\xi} \tag{8}$$

where Ω^d is the random space that the ξ variables span, and $p(\boldsymbol{\xi}) = p_1(\xi_1)\cdot p_2(\xi_2)\cdot\ldots\cdot p_d(\xi_d)$ is the joint probability density function. Consequently, we have

$$\left\langle \Psi_i(\boldsymbol{\xi}), \Psi_j(\boldsymbol{\xi})\right\rangle = \left\|\Psi_i(\boldsymbol{\xi})\right\|^2 \delta_{ij} \tag{9}$$

where $\left\|\Psi_i(\boldsymbol{\xi})\right\|^2 = \left\langle \Psi_i(\boldsymbol{\xi}), \Psi_i(\boldsymbol{\xi})\right\rangle$ and δ_{ij} is the Kronecker delta.

In this paper, we are mainly concerned with uncertainties pertinent to the geometric properties of the investigated crack. In essence, the ξ variables are considered to be uniformly distributed with $\xi_i \in [-1, 1]$, $i = 1, \ldots, d$ (hence, $\Omega^d = [-1, 1]^d$ and $p(\boldsymbol{\xi}) = 0.5^d$), which are mapped to the original – geometric – variables via linear functions. For instance, if L is a geometric dimension of the crack within the range $[L_{\min}, L_{\max}]$ and associated with the ξ_m variable, then the following formula is used:

$$L(\xi_m) = \frac{L_{\max}+L_{\min}}{2} + \frac{L_{\max}-L_{\min}}{2}\xi_m \tag{10}$$

Note that, due to the uniformly distributed random variables, the optimal choice for the basis functions is to use Legendre polynomials for their construction [13].

4. Calculation of Expansion Coefficients and Extraction of Statistics

The $C_\ell^U(\mathbf{r})$ coefficients involved in the PC expansions can be calculated in a non-intrusive fashion (i.e. without modifying the deterministic solver), through projection on every basis function, via

$$C_k^U(\mathbf{r}) = \frac{\left\langle \Delta U(\mathbf{r},\boldsymbol{\xi}), \Psi_k(\boldsymbol{\xi})\right\rangle}{\left\|\Psi_k(\boldsymbol{\xi})\right\|^2},\ k = 0,\ldots,P \tag{11}$$

Evidently, the above formula requires the implementation of a quadrature rule for the computation of the numerators (the denumerators can be obtained analytically). The numerical computation of integrals is a subject of general interest, and several techniques have been developed till today. Normally, a quadrature rule is applied in the form

$$\left\langle \Delta U(\mathbf{r},\boldsymbol{\xi}), \Psi_k(\boldsymbol{\xi})\right\rangle \simeq \sum_{i=1}^{N} w\left(\boldsymbol{\xi}^{(i)}\right)\Delta U\left(\mathbf{r},\boldsymbol{\xi}^{(i)}\right)\Psi_k\left(\boldsymbol{\xi}^{(i)}\right)p\left(\boldsymbol{\xi}^{(i)}\right) \tag{12}$$

where $\boldsymbol{\xi}^{(i)}$ denotes a pre-determined set of nodes on Ω^d and $w(\boldsymbol{\xi}^{(i)})$ is the corresponding set of weights. In this paper, we consider integration rules that are based on the Kronrod-Patterson (KP) nodal sets. For multi-dimensional problems, sparse grids based on the Smolyak algorithm [14] constitute more attractive choices than full – tensor based – grids, as they are capable of providing accurate predictions with reduced sets of nodes and, therefore, result in smaller

computational times (recall that each node in the random space corresponds to a full-wave simulation). In particular, we perform calculations based on delayed KP nodes [16], which means that the quadrature nodes are repeated for certain construction levels of the grid, controlling the growth of the grid size.

More specifically, when performing integration on sparse grids, one needs to evaluate the integrated quantity on the nodes determined by

$$\Theta = \bigcup_{k+1\le|\mathbf{i}|\le k+d} \left(\Theta_1^{i_1}\times\Theta_1^{i_2}\times\ldots\times\Theta_1^{i_d}\right) \tag{13}$$

where the parameter k denotes the level of construction of the Smolyak grid, and $\Theta_1^i = \{\theta_1^i, \theta_2^i, \ldots, \theta_{m_i}^i\}$ denotes the set of m_i nodes of the 1D quadrature rule. Some representative examples of 2D sparse grids are shown in Fig. 2, and compared against a full grid. The corresponding quadrature rule is then described by

$$I \simeq \sum_{k+1\le|\mathbf{i}|\le k+d} (-1)^{k+d-|\mathbf{i}|}\binom{d-1}{k+d-|\mathbf{i}|}\left(U^{i_1}\otimes U^{i_2}\otimes\ldots\otimes U^{i_d}\right) \tag{14}$$

where U^i denotes the i-th level 1D quadrature rule. Evidently, (14) considers specific combinations of product formulae, in contrast to the tensor product

$$I_{\text{full}} \simeq U^{i_1}\otimes U^{i_2}\otimes\ldots\otimes U^{i_d} \tag{15}$$

which involves $m_{i_1} m_{i_2} \ldots m_{i_d}$ nodes.

After performing the necessary projections, fundamental statistical properties of the impedance change, as described by the expected value and the variance, are deduced from the PC coefficients:

$$\mathrm{E}[\Delta U] = C_0^U \tag{16}$$

$$\mathrm{var}[\Delta U] = \sum_{k=1}^{P}\left(C_k^U\right)^2 \left\|\Psi_k(\xi)\right\|^2 \tag{17}$$

It is stressed that the PC expansions constitute a complete representation of the corresponding random quantities, providing more information than just (16), (17), as will be verified by the numerical results.

5. Matlab Scripting

To facilitate consecutive impedance evaluations, which are necessary both for MC and PC approaches, the COMSOL® model of the investigated problem is exported as a Matlab function, whose input variables are the coil's position and the geometric dimensions of the plate's defect. For this reason, the function's

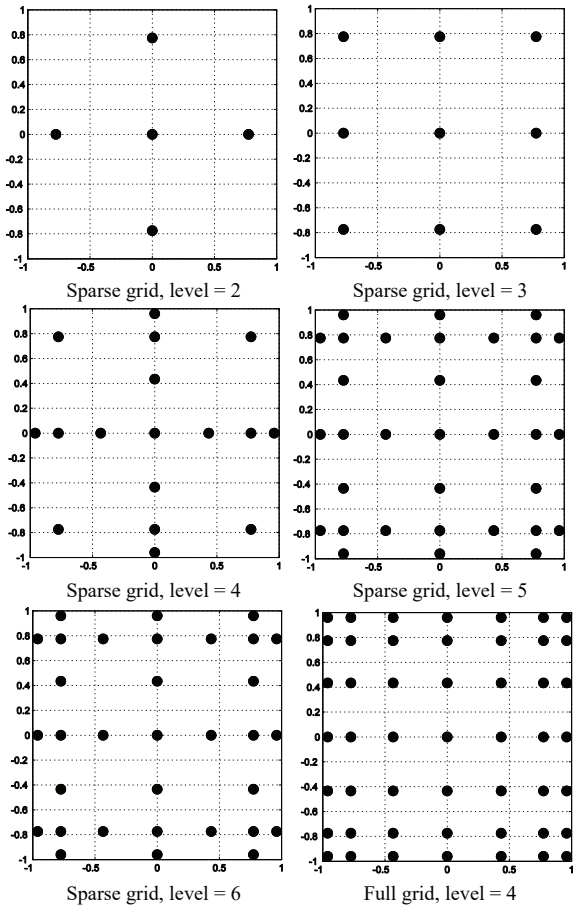

Figure 2. Comparison of various two-dimensional sparse grids with a full grid.

first line is formulated as

```
function out = coil_defect(m,xc,yc,zc)
```

and the corresponding directives for the inputs are modified, as following:

```
model.param.set('m',[num2str(m),
'[mm]'], 'movement');
model.param.set('xc',[num2str(xc),
'[mm]'], 'x dimension of crack');
model.param.set('yc',[num2str(yc),
'[mm]'], 'y dimension of crack');
model.param.set('zc',[num2str(zc),
'[mm]'], 'z dimension of crack');
```

Then, two similar scripts are developed, one for the MC studies and one for conducting the simulations required by the PC expansions. In the former case, the values of the uniformly-distributed parameters ξ are obtained via

```
xi = 2*rand(samples,3)-1;
```

where `samples` denotes the selected number of successive evaluations (normally, of the order of thou-

sands). In the case of the PC approach, the ξ values correspond to specific integration nodes and are determined via

```
[nodes, wgts] = nwspgr('KPU',3,level);
xi = 2*nodes-1;
```

where the `nwspgr.m` function is taken from [17], and produces, according to the above formulation, 3D sparse grids based on delayed KP nodal sets.

6. Numerical Results

We have experimented with various combinations of random variables, value ranges, etc., and we present a fraction of these results. Specifically, the problem under study considers mean values of the coil's x_c, y_c, z_c dimensions equal to 0.5 mm, 10 mm, and 5 mm, respectively, with deviations of the order of ±10% around the aforementioned averages. The changes in the coil's impedance are calculated for coil positions in the range 0-20 mm – with respect to the central point of the defect – along the y-direction. We initially gather reference simulation results by employing the MC approach for 2000 samples (each "sample" actually corresponds to the impedance changes at all coil positions, with spatial step of 1 mm). This number of samples is expected to produce quite reliable outcomes, although several thousands of simulations are usually required, in order to ensure very accurate results. Then, another (smaller) set of simulations is performed, according to the selected level of sparse-grid quadrature, and the PC expansions of the coil's impedance components are computed as described earlier, providing a complete statistical description of the examined variables.

First, the mean value and the standard deviation of the ΔR and ΔX components are examined, as a function of the coil's position. The comparison between MC and PC calculations is depicted in Fig. 3. Regarding the mean-value estimates, excellent agreement can be observed, even when a low-level sparse grid with only 19 nodes and just first-order (p = 1) basis functions are utilized. The reliable computation of the standard deviation appears to be more challenging. Nevertheless, the good agreement in Fig. 3 is obtained considering an 87-node grid and second-order polynomial approximations (p = 2). One may observe that the maximum mean values appear when the coil is positioned at approximately 7 mm from the central point of the geometry. Furthermore, the shapes of the standard-deviation curves appear to

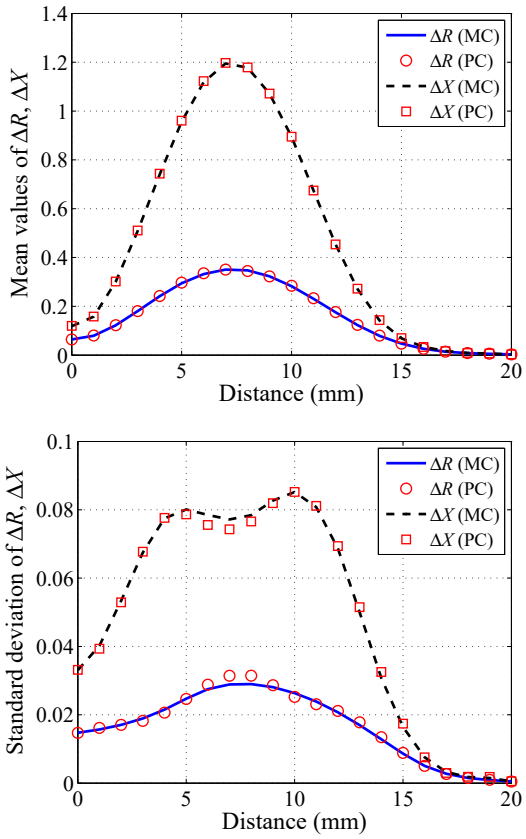

Figure 3. Mean value (top) and standard deviation (bottom) of the change in coil's impedance, as a function of the coil position.

be quite different for ΔR and ΔX, with the pattern of the coil's reactance exhibiting the most significant values in the range 4-11 mm.

Next, the probability density functions (PDFs) that completely describe the statistics of the coil's impedance change at a distance of 7 mm (which corresponds to the position of the maximum expected value, according to Fig. 3) are estimated via the PC expansions and compared against the MC results. Note that the PC-based PDFs are computed, after gathering a large amount of samples (150,000) within a matter of seconds, by applying a MC technique directly to the PC series. The latter are determined using Smolyak grids with accuracy level equal to six. As expected, Fig. 3 verifies that low-order polynomial approximations, although sufficient for mean-value estimations, do not capture reliably all the properties of the corresponding distributions. In the case of ΔR, setting p = 3 produces better results than the lower-order expansions, while setting p = 2 or 3 appear to provide similar accuracy levels in the case of ΔX.

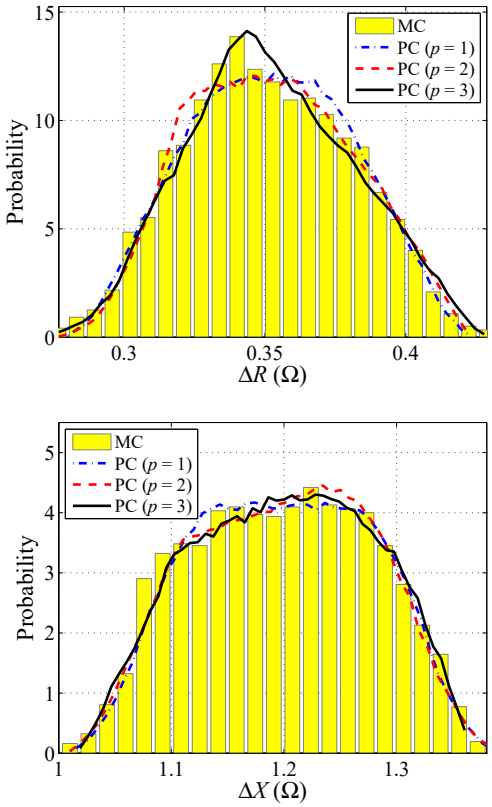

Figure 4. Computed PDFs corresponding to ΔR (top) and ΔX (bottom) at a distance of 7 mm.

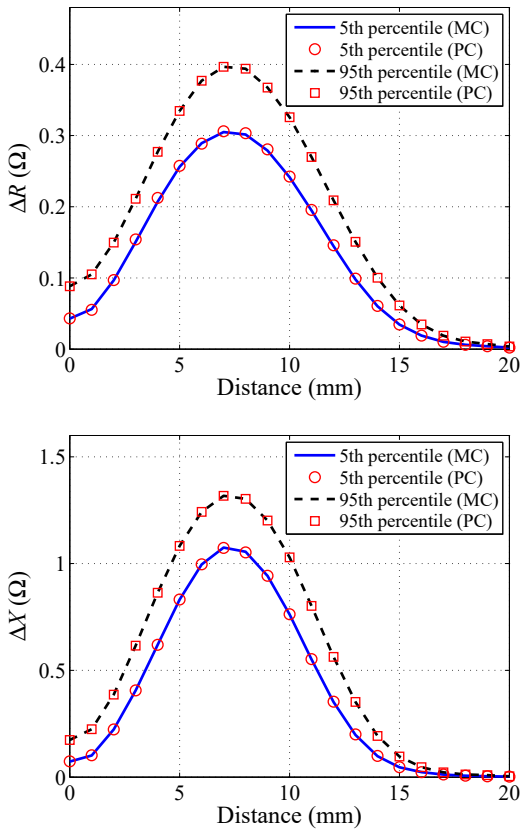

Figure 5. Upper and lower bounds of ΔR and ΔX, represented by the 95th and 5th percentiles.

Another result that validates the reliability of the PC methodology pertains to the computation of the lower and upper bounds of the changes in the coil's impedance. These bounds are represented here by the 5th and the 95th percentiles, which can be computed from the corresponding PDFs. Figure 5 displays the comparison between the reference curves and the PC-based results, when $p = 3$ and an accuracy level of six is selected for the quadrature rule. The depicted outcomes reveal an almost excellent agreement, which is to be expected, given the small differences between the calculated PDFs mentioned earlier. In the case of ΔR, the most pronounced distance between the two bounds is observed at 8 mm, where the corresponding values cover the interval 0.3034 – 0.3939 Ω, while the corresponding interval in the case of ΔX is 0.5524 – 0.8018 Ω and is observed at 11 mm.

Finally, a sensitivity analysis is performed, to determine the influence of each of the geometric parameters on the results, without carrying out any extra simulations. The necessary information is extracted from the Sobol indices, which are directly computed from the available PC coefficients:

$$S_v^U \simeq \frac{\sum_{\ell \in K_v} \left(C_\ell^U\right)^2 \left\|\Psi_\ell\right\|^2}{\sum_{\ell=1}^{P} \left(C_\ell^U\right)^2 \left\|\Psi_\ell\right\|^2} \tag{18}$$

where K_v stands for the following set of indices:

$$K_v = \left\{ k \in \{1,\ldots,P\} : \Psi_k(\boldsymbol{\xi}) = \prod_{i=1}^{|v|} \psi_{a_i^k}\left(\xi_{v_i}\right) \right\} \tag{19}$$

For the problem under investigation, v may correspond to {1}, {2}, {3}, {1,2}, {1,3}, {2,3}, and {1,2,3}, hence there exist seven Sobol indices, with the first three ones denoting first-order contributions. Figure 6 displays the contribution of each of the three geometric parameters on the change of the resistance and reactance, as a function of the coil's position. Evidently, the variability of the output is mainly due to the second geometric parameter (y_c), while the other two dimensions appear to play a less prominent role. In fact, their contribution becomes more significant at positions 6-8 mm, with z_c being more influent-

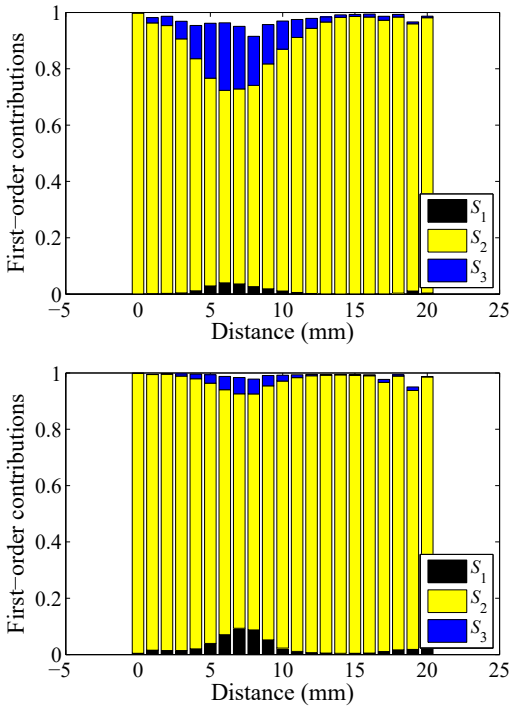

Figure 6. Calculation of the first-order Sobol indices, regarding the real part (top) and the imaginary part (bottom) of the coil's impedance change.

ial for the real part of the coil's impedance, rather than ΔX. The depicted results have been computed assuming third-order polynomial expansions and Smolyak grid of level six. Note that the sum of the three Sobol indices at each position is less than 1, as higher-order contributions have not been included (the sum of all Sobol indices is unity).

7. Conclusions

By exploiting the potential of PC representations and sparse-grid quadrature, we have used the deterministic FEM solver of COMSOL® for the investigation of stochastic eddy-current testing problems. Unlike MC methodologies, whose slow convergence suggest long simulation times, our approach provides reliable statistical information using a fraction of the aforementioned computational requirements. As the numerical results have pointed out clearly, perturbations of a defect's geometric properties are likely to have non-trivial impact on the coil's impedance, which constitutes the main criterion for defect detection.

References

1. B. A. Auld and J. C. Moulder, Review of advances in quantitative eddy current nondestructive evaluation, *J. Nondestruct. Eval.*, **18** (1), 3-36 (1999).
2. A. Sophian, G. Y. Tian, D. Taylor, and J. Rudlin, Electromagnetic and eddy current NDT: a review, *Insight - Non-Destruct. Test. & Cond. Monitor.*, **43** (5), 1-5 (2001).
3. F. Matsuoka and A. Kameari, Calculation of three dimensional eddy current by FEM-BEM coupling method, *IEEE Trans. Magn.*, **24** (1), 182-185 (1988).
4. J. R. Bowler, Eddy-current interaction with an ideal crack. I. The forward problem, *J. Appl. Phys.*, **75** (12), 8128-8137 (1994).
5. J. R. Bowler, Y. Yoshida, and N. Harfield, Vector-potential boundary-integral evaluation of eddy-current interaction with a crack, *IEEE Trans. Magn.*, **33** (5), 4287-4294 (1997).
6. R. Albanese, G. Rubinacci, and F. Villone, An integral computational model for crack simulation and detection via eddy currents, *J. Comp. Phys.*, **152**, 736-755 (1999).
7. M. Tanaka and H. Tsuboi, Finite element model of natural crack in eddy current testing problem, *IEEE Trans. Magn.*, **37** (5), 3125-3128 (2001).
8. T. Theodoulidis, Developments in efficiently modelling eddy current testing of narrow cracks, *NDT&E Int.*, **43**, 591-598 (2010).
9. T. Theodoulidis, N. Poulakis, A. Dragogias, Rapid computation of eddy current signals from narrow cracks, *NDT&E Int.*, **43**, 13-19 (2010).
10. L. Santandrea and Y. Le Bihan, Using COMSOL-multiphysics in an eddy current non-destructive testing context, *Proceedings of the COMSOL Conference*, Paris (2010).
11. X. Jiang, P. Li, and W. Zheng, Eddy current model for nondestructive evaluation with thin cracks, *SIAM J. Sci. Comput.*, **38** (2), A973-A996 (2016).
12. M. N.O. Sadiku, *Monte Carlo methods for electromagnetics*, CRC Press, Boca Raton, FL: USA (2009).
13. D. Xiu and G. E. Karniadakis, The Wiener–Askey polynomial chaos for stochastic differential equations, *SIAM J. Sci. Comp.*, **24** (2), 619-644 (2002).
14. S. Smolyak, Quadrature and interpolation formulas for tensor products of certain classes of functions, *Sov. Math., Dokl.*, **4**, 240-243 (1963).
15. R. Gaignaire, R. Scorretti, R. V. Sabariego, and C. Geuzaine, Stochastic uncertainty quantification of eddy currents in the human body by polynomial chaos decomposition, *IEEE Trans. Magn.*, **48**, 451-454 (2012).
16. K. Petras, Smolyak cubature of given polynomial degree with few nodes for increasing dimension, *Num. Math.*, **93**, 729-753 (2003).
17. http://www.sparse-grids.de/